

Nucleation control of diamond synthesized by microwave plasma CVD on cemented carbide substrate

H. ITOH, T. OSAKI, H. IWAHARA

Synthetic Crystal Research Laboratory, School of Engineering, Nagoya University, Furo-cho, Chikusa-ku, Nagoya 464-01 Japan

H. SAKAMOTO

Sigma Coating Engineering, 21-33, Moriganishi-cho, Uzumasa, Ukyo-ku, Kyoto 616, Japan

Diamond was coated on to cemented carbide substrate by microwave plasma CVD, in which nucleation control of diamond crystals was investigated under constant deposition conditions; total pressure 30 torr, CH_4 flow rate 1 ml min^{-1} , H_2 flow rate 199 ml min^{-1} and microwave power 550 W. Nucleation tends to occur selectively on the edge part of WC grains of the cemented carbide substrate with coarse WC grain size of about $1 \mu\text{m}$, where the nucleation density was $9 \times 10^6 \text{ cm}^{-2}$. The density increased to about $5 \times 10^7 \text{ cm}^{-2}$ when using a fine-grained substrate (WC grain size $\sim 0.5 \mu\text{m}$). A considerably enhanced nucleation was observed by introducing a number of fine microflaws on to the substrate surface. Microflawing treatment with diamond fine powder (grain size $0\text{--}1/4 \mu\text{m}$) suspended in an ultrasonic cleaner bath was effective for increasing the diamond nucleation density up to $5 \times 10^8 \text{ cm}^{-2}$. The grain size of grown diamond crystals decreased with increasing microflawing time.

1. Introduction

Diamond film is needed for application to coated cutting tools for precision working of nonferrous substances [1–3]. The subject requires urgent investigation of a practical application of chemically vapour deposited (CVD) diamond coatings to increase the toughness and adherence of the diamond film. The first step to attain this goal is to control the nucleation process of diamond and to increase the nucleation density [4–6], which would lead to the formation of fine-grained diamond film. It is often pointed out in the case of CVD of diamond on a silicon substrate [7–12], that microflaws on the substrate surface might play an essential role in nucleation of diamond. An appropriate selection of substrate microstructure or pretreatment of the substrate will also be necessary in the CVD of diamond on cemented carbide substrate, so that the nucleation density can be increased and to improve the film microstructure [2, 13].

In the present work, diamond was synthesized by microwave plasma-enhanced CVD in the $\text{CH}_4\text{--H}_2$ reactant system using the cemented carbide (WC–Co system) as substrate. Effects of the microstructure of the cemented carbide substrate and a microflawing pretreatment of the substrate surface were investigated in relation to the nucleation of diamond crystals.

2. Experimental procedure

Fig. 1 shows the microwave plasma CVD apparatus

for synthesis of diamond which was designed by Sigma Coating Engineering. Microwave power (frequency 2.45 GHz, power 0.1–1.5 kW) was applied to the vertical quartz reactor tube (i.d. 48 mm), in which a cemented carbide substrate (WC–Co triangular chip, 17 mm each side length, 4.6 mm thick) was mounted on a quartz pedestal. A mixture of CH_4 and H_2 gases

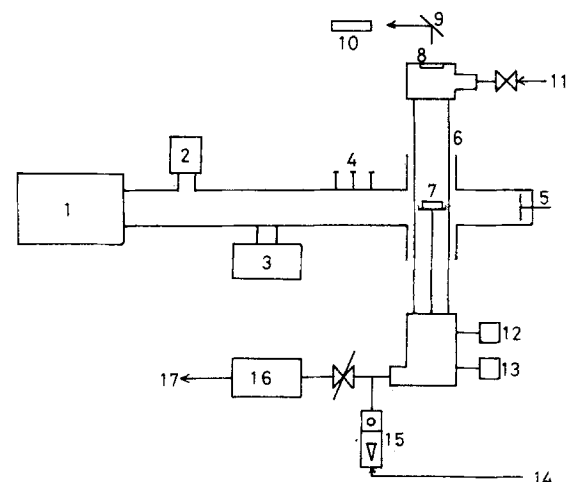


Figure 1 Microwave plasma CVD apparatus for diamond coating. 1, Microwave generator; 2, isolator; 3, power monitor; 4, tuner; 5, plunger; 6, quartz reactor; 7, substrate; 8, observation window; 9, mirror; 10, optical pyrometer; 11, $\text{CH}_4 + \text{H}_2$; 12, Geissler tube; 13, vacuum gauge; 14, N_2 ; 15, flow meter; 16, rotary pump; 17, exhaust.

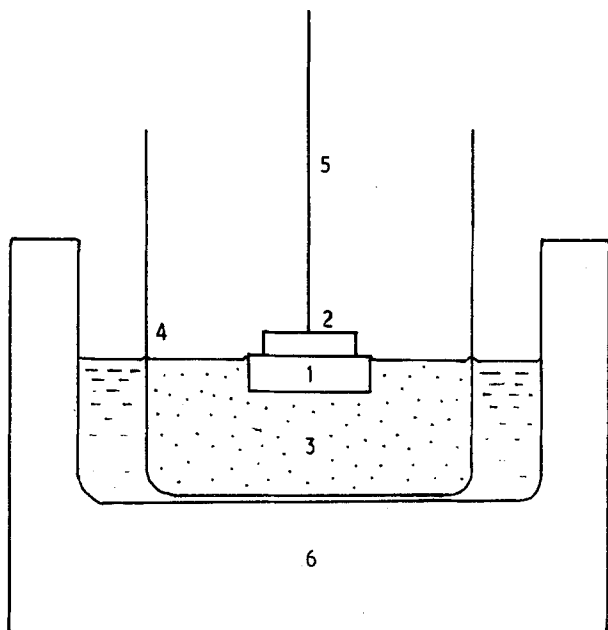


Figure 2 Ultrasonic microflawing equipment of cemented carbide substrate. 1, Specimen; 2, magnet; 3, diamond powder in ethanol; 4, beaker; 5, wire; 6, ultrasonic cleaner bath.

was introduced to the upper part of the reactor. The total pressure of the reactor was modulated by the leak valve and the flowmeter of nitrogen gas. The substrate temperature was measured by an optical pyrometer through the observation window attached to the top. Coarse or fine-grained WC-Co substrate was polished by diamond powder (grain size 1 μm).

Microflawing of the polished substrate surface with diamond powder was carried out for 0–60 min in a beaker dipped in an ultrasonic cleaner bath (power 18 W), as shown in Fig. 2. Diamond powder (1 g) having three different grain sizes (0– $\frac{1}{4}$ μm , 5–10 μm and 40–60 μm) was dispersed in 20 ml ethanol. The substrate, which was suspended by using a magnet, was microflawed in the diamond-dispersed ethanol.

The deposits formed by CVD were analysed by X-ray diffraction and laser-Raman spectrometry. The substrate surface was observed by scanning electron microscopy (SEM) before and after the CVD treatment. The nucleation density was calculated by counting the number of nucleated diamond crystals in a unit area on a scanning electron micrograph. The surface roughness was measured by the roughness meter using a contact probe technique.

3. Results and discussion

3.1. Nucleation of diamond on a cemented carbide substrate

Diamond crystals which have euhedral habits were deposited on a cemented carbide substrate under the following conditions: total pressure 30 torr, CH_4 flow rate 1 ml min^{-1} , H_2 flow rate 199 ml min^{-1} , microwave power 550 W, substrate temperature 870–900 $^\circ\text{C}$ and reaction time 5 h. Fig. 3a and b show X-ray diffraction patterns of the surface of specimens (a) before and (b) after the CVD treatment. All the diffraction lines in Fig. 3a correspond to those of

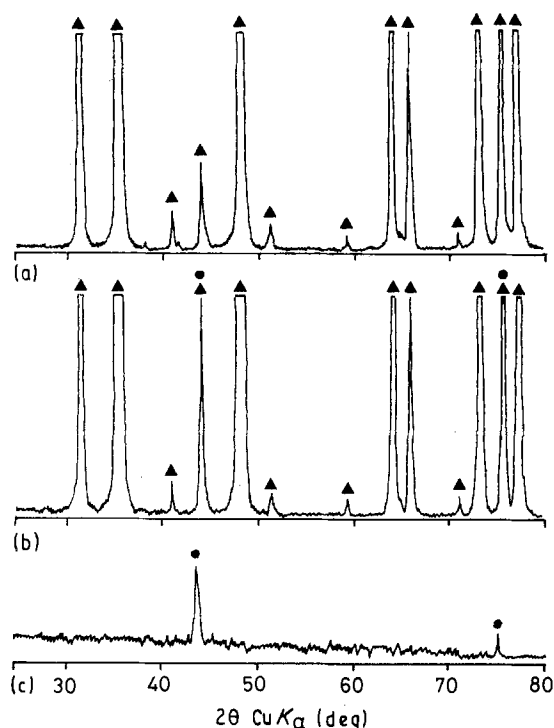


Figure 3 X-ray diffraction patterns of specimen surface (a) before and (b) after CVD treatment, and of (c) the deposits separated from the substrate. (●) Diamond, (▲) cemented carbide. Deposition conditions: total pressure 30 torr, CH_4 flow rate 1 ml min^{-1} , H_2 199 ml min^{-1} , power 550 W, reaction time 5 h, ultrasonic microflawing with 5–10 μm diamond grains for 15 min.

cemented carbide substrate (WC, Co and trace of unknown additives). After the CVD treatments (see Fig. 3b), the diffraction lines of 111 at $2\theta = 43.9^\circ$ and 220 at $2\theta = 75.3^\circ$ can be observed, although both lines overlap with those of cemented carbide. No graphitic or amorphous carbonaceous deposit was identified. Fig. 3c shows the X-ray diffraction pattern of some pieces of deposit peeled off from the substrate. Crystalline diamond can be identified with no detection of non-diamond components.

Fig. 4 shows a Raman spectrum of the coated specimen obtained under the same conditions as in Fig. 3. A single peak at 1334 cm^{-1} corresponds to that of diamond [8]. Other peaks attributed to graphite

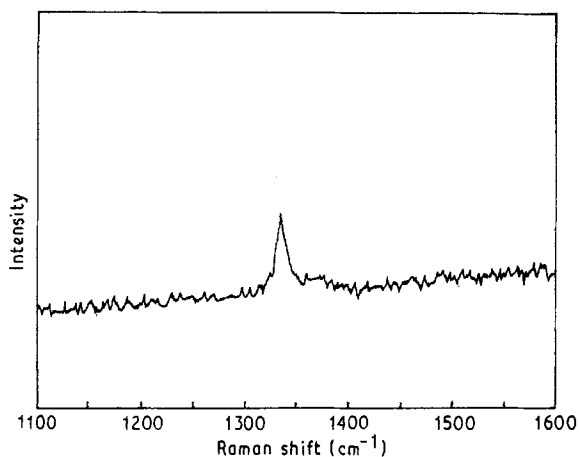


Figure 4 Raman spectrum of the coated diamond specimen which is the same as that in Fig. 3b.

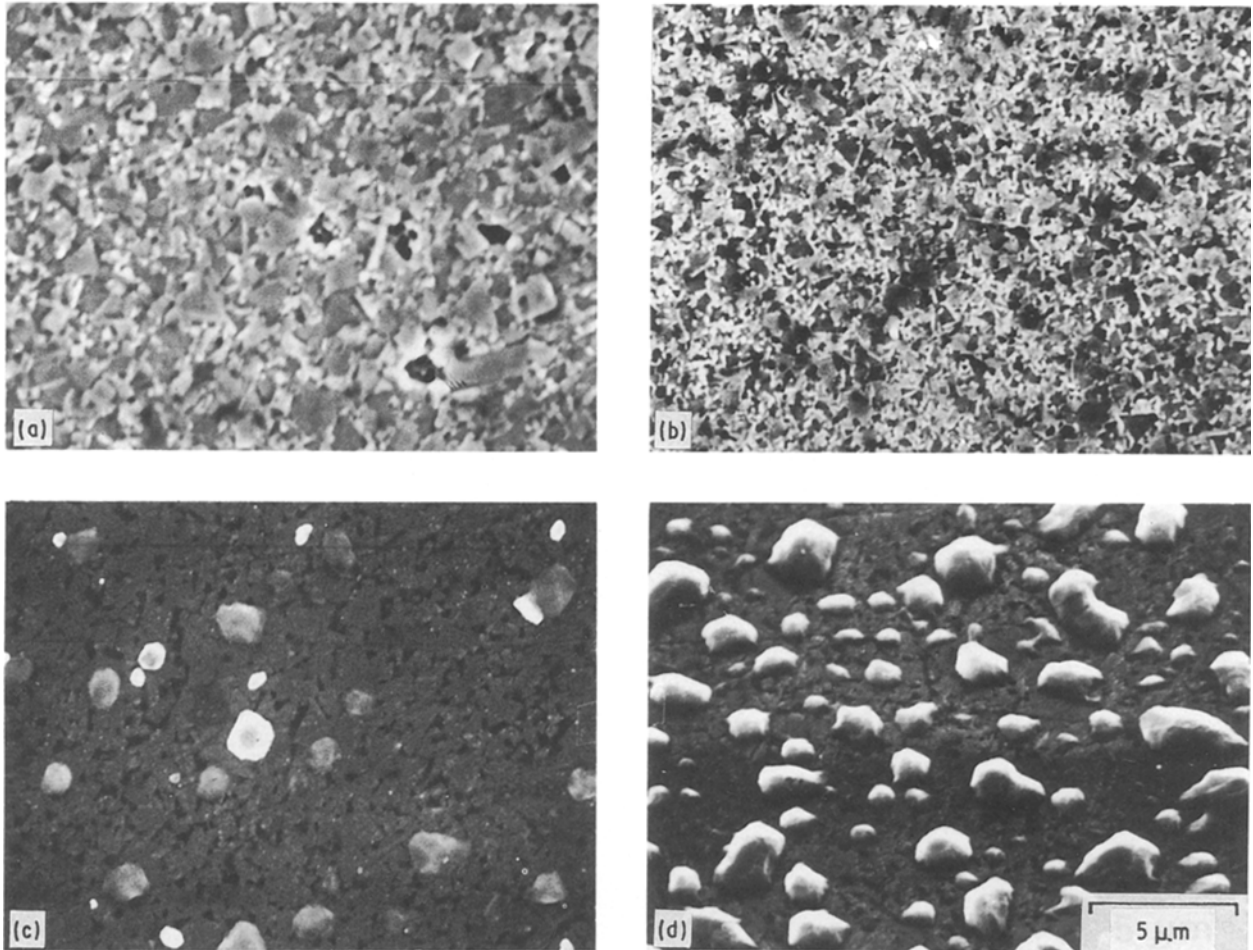


Figure 5 Scanning electron micrographs of the specimen surface before the CVD treatment of (a) coarse-grained substrate and (b) fine-grained substrate, and after the CVD treatment of (c) coarse-grained substrate and (d) fine-grained substrate.

(1580 cm^{-1}) and amorphous carbon ($1360\text{--}1550 \text{ cm}^{-1}$) cannot be seen. It is concluded that the deposit formed under the above conditions is single-phase diamond. All the following experiments were carried out under these optimum deposition conditions.

Fig. 5 shows the influence of WC grain size in cemented carbide on the nucleation of diamond, where (a) and (b) are scanning electron micrographs of coarse-grained (grain size $1 \mu\text{m}$) and fine-grained (grain size $0.5 \mu\text{m}$) substrates, respectively, which were etched in Murakami reagent ($\text{K}_3[\text{Fe}(\text{CN})_6]:\text{KOH}:\text{H}_2\text{O} = 1:1:10$) before CVD treatment. It was found from the micrographs (c, d) of the specimens which were obtained by CVD treatment for 1 h, that the nucleation density of the fine-grained specimen ($5 \times 10^7 \text{ cm}^{-2}$) was about five times greater than that of the coarse-grained specimen (nucleation density $9 \times 10^6 \text{ cm}^{-2}$). In order to examine the selectivity for nucleation sites on the polished substrate, a nucleation experiment (reaction time 1 h) was carried out using a coarser grained specimen (WC grain size $\sim 5 \mu\text{m}$). Fig. 6 shows a scanning electron micrograph of the nucleated diamond grains on the cemented carbide substrate, which was etched by Murakami reagent after the CVD treatment. Apparently, diamond nuclei favours deposition on the edge of the WC grains that includes the grain-boundary region between WC phase and Co phase.

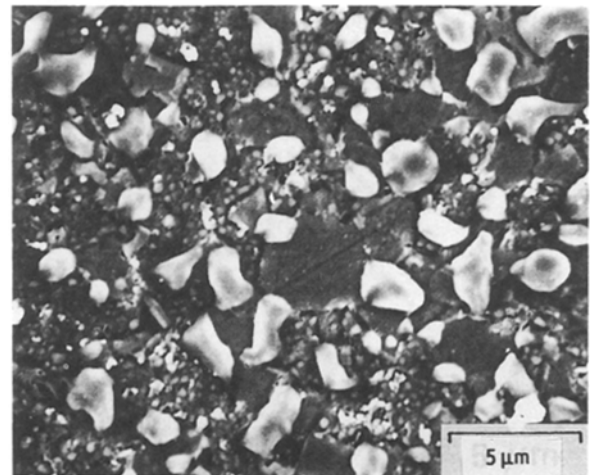


Figure 6 Scanning electron micrograph of the nucleated diamond grains on coarse-grained cemented carbide substrate.

3.2. Effects of microflawing the substrate surface on diamond nucleation

The microflawing effects on diamond nucleation were investigated preliminarily for silicon (100) substrate surface by means of scratching with abrasive powders (SiO_2 , Al_2O_3 , etc.) and SiC emery paper, or by means of microflawing the substrate surface by collision of Al_2O_3 or diamond powder in an ultrasonic field.

Among the above techniques, an ultrasonic microflawing treatment with diamond powder was the most effective in enhancing the nucleation density.

Fig. 7 shows a relationship between nucleation density and grain size of the microflawing diamond powder, where the microflawing time and CVD reaction time are kept constant at 15 min and 1 h, respectively. Compared with the nucleation density ($9 \times 10^6 \text{ cm}^{-2}$), as shown in Fig. 5a) in the case without microflawing, the density increased remarkably to $5 \times 10^8 \text{ cm}^{-2}$ when using diamond powder of $0\text{--}\frac{1}{4} \mu\text{m}$ grain size. Fig. 8 shows a scanning electron micrograph of the diamond particles nucleated on the coarse-grained cemented carbide substrate. A dense and homogeneous distribution of diamond crystals was found to extend to the whole area of the substrate. Fig. 7 represents that the nucleation density tends to decrease with increasing grain size of microflawing diamond powder and the density was $4 \times 10^7 \text{ cm}^{-2}$ when using the grain size of $40\text{--}60 \mu\text{m}$. This suggests that the finer the microflaws generated on the substrate, the greater is the nucleation density. Finer

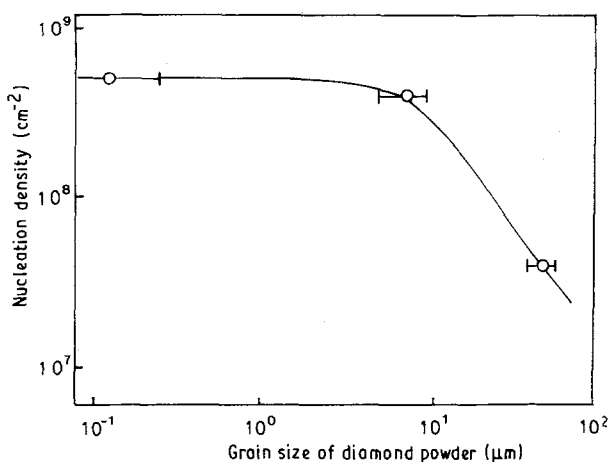


Figure 7 Relationship between nucleation density and the grain size of microflawing diamond powder. Microflawing time 15 min, CVD treatment time 1 h.

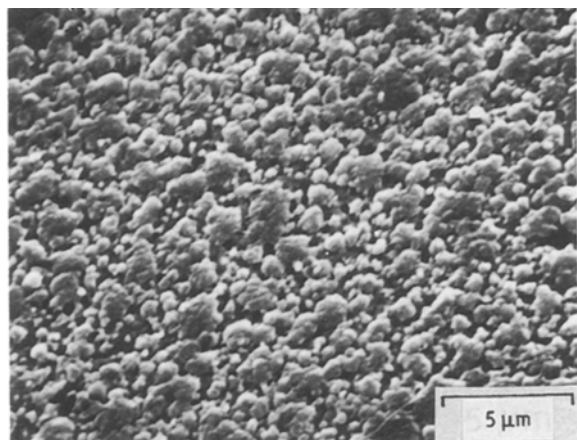


Figure 8 Scanning electron micrograph of the diamond particles nucleated on microflawed substrate. Microflawed diamond grain size $0\text{--}\frac{1}{4} \mu\text{m}$, CVD treatment time 1 h.

microflaws given by $0\text{--}\frac{1}{4} \mu\text{m}$ grains are considered to provide the activated nucleation sites of diamond. As the grain size of microflawing diamond decreases, the number of grains in a given amount of diamond powder (1 g) would increase. This results in an increase in the collision frequency of diamond grains and hence in the number of nucleation sites.

Fig. 9 shows the effect of microflawing time on diamond nucleation, where the microflawing diamond grain size and CVD reaction time were kept constant at $5\text{--}10 \mu\text{m}$ and 1 h, respectively. The nucleation density for microflawing time of 15, 30 and 60 min was found to be 3×10^8 , 2×10^8 , and $3 \times 10^8 \text{ cm}^{-2}$, respectively. The grain size of nucleated diamond was about $0.8 \mu\text{m}$ for the microflawing time of 15 and 30 min, while the grain size decreased to about $0.4 \mu\text{m}$ for 60 min. The growth rate of diamond nuclei seems to be affected by the size and shape of microflaws which would vary with microflawing time.

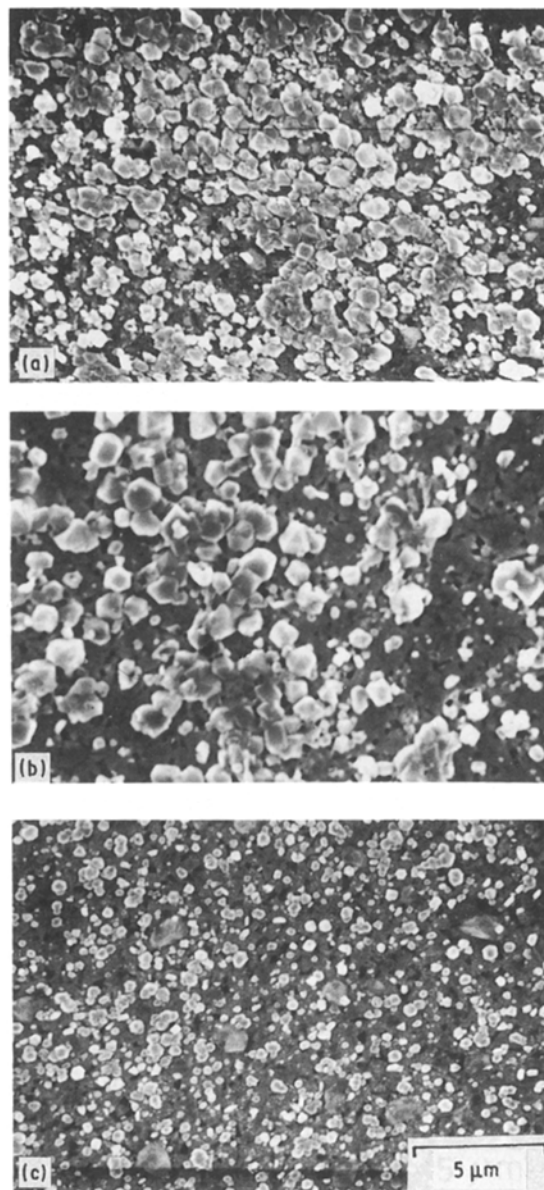


Figure 9 Effect of microflawing time on diamond nucleation. Microflawing time: (a) 15 min, (b) 30 min, (c) 60 min. Microflawing diamond grain size $5\text{--}10 \mu\text{m}$, CVD treatment time 1 h.

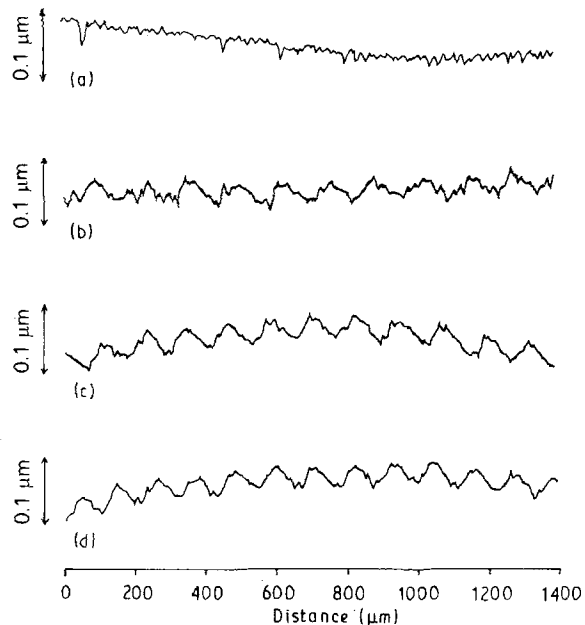


Figure 10 Profile of the roughness of the substrate surface. (a) As-polished, (b) microflawed by $0\text{--}\frac{1}{4}\mu\text{m}$ grain for 15 min, (c) microflawed by $40\text{--}60\mu\text{m}$ grain for 15 min, (d) microflawed by $0\text{--}\frac{1}{4}\mu\text{m}$ grain for 60 min.

Fig. 10 shows line profiles of the surface roughness of the substrate with and without microflawing treatment. The as-polished surface is relatively smooth as a whole (see Fig. 10a), but has a few irregular flaws. In

the specimens (Fig. 10b–d) subjected to the microflawing treatment, a periodic ruggedness with an amplitude of about 50 nm can be observed in every $100\mu\text{m}$ length. In a periodic flaw, finer microflaws can be seen in which the separations between them would be submicrometre, although the shape and size of each microflaw is difficult to distinguish by this roughness meter. The roughness appears to become sharper as the grain size of microflawing diamond grains increases (compare b and c). On the other hand, the roughness appears smooth on increasing the microflawing time up to 60 min. This information which is insufficient to visualize, does however, give valuable suggestions concerning the microflawing effects on diamond nucleation and subsequent crystal growth. An approximate distance between microflaws is estimated to be about $0.5\mu\text{m}$ by calculation from the nucleation density of the order of $5 \times 10^8\text{ cm}^{-2}$.

Fig. 11 shows the nucleation and growth process of diamond crystals as a function of CVD treatment time, where the coarse-grained cemented carbide substrate was microflawed by ultrasonic treatment for 15 min using diamond powder with a grain size of $5\text{--}10\mu\text{m}$. A homogeneous distribution of small nuclei can be seen after a CVD treatment time of 5 min as shown in Fig. 11a, where the nucleation density is $3 \times 10^8\text{ cm}^{-2}$. Nucleation continues up to about $\frac{1}{2}\text{--}1\text{ h}$ (see Fig. 11b and c) and attains a density of $5 \times 10^8\text{ cm}^{-2}$. Growth of diamond nuclei prevails after

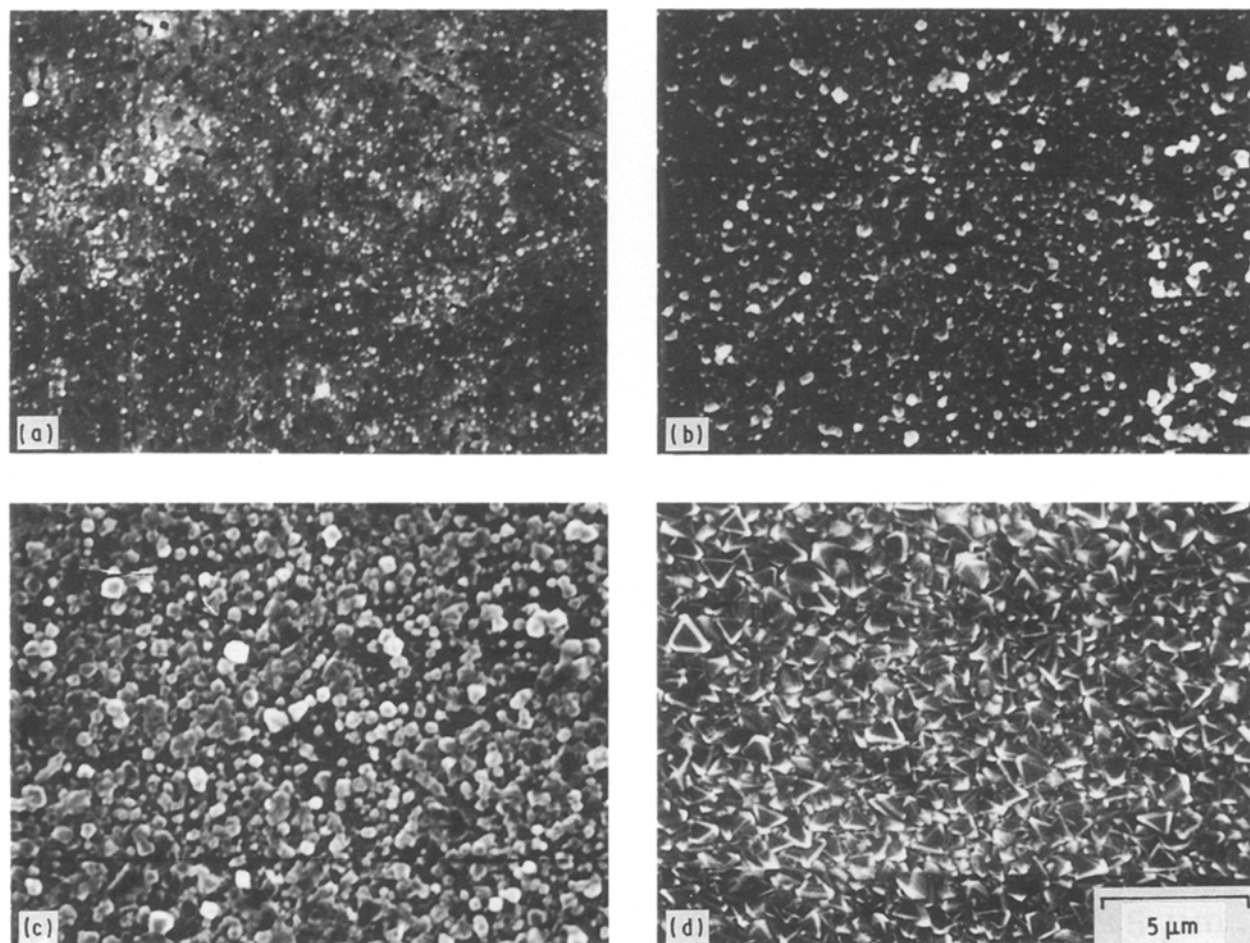


Figure 11 Nucleation and growth process of diamond as a function of CVD treatment time. (a) 5 min, (b) 30 min, (c) 1 h, (d) 5 h.

1–2 h which leads to the appearance of euhedral habits followed by the contact and aggregation of growing diamond crystals and finally to the formation of a fine-grained diamond film, about 0.5 μm thick, as shown in Fig. 11d.

4. Conclusions

Nucleation of diamond in the microwave plasma CVD was controlled by an appropriate selection of cemented carbide substrate and by microflawing pretreatment of the substrate in an ultrasonic field. The following conclusions were obtained under the plasma CVD conditions investigated: total pressure 30 torr, CH_4 flow rate 1 ml min^{-1} , H_2 flow rate 199 ml min^{-1} and microwave power 550 W.

1. The nucleation density of the coarse-grained cemented carbide (WC grain size $1 \mu\text{m}$) was $9 \times 10^6 \text{ cm}^{-2}$, while that on fine-grained substrate (WC grain size $0.5 \mu\text{m}$) was $5 \times 10^7 \text{ cm}^{-2}$. Nucleation of diamond occurs selectively on the edge of WC grains.

2. Microflawing the substrate surface by an ultrasonic treatment using diamond powder suspended in ethanol was very effective in enhancing the nucleation density up to $5 \times 10^8 \text{ cm}^{-2}$.

3. The nucleation density increased with decreasing grain size of the microflawing diamond powder. The grain size of nucleated diamond decreased with microflawing time. Finer microflaws are considered to provide active nucleation sites for diamond.

4. Uniform nucleation occurs within the CVD treatment time of $\frac{1}{2}$ –1 h and attains a nucleation

density of the order of 10^8 cm^{-2} , then followed by growth of diamond and subsequent formation of a fine-grained diamond film.

References

1. K. E. SPEAR, *J. Amer. Ceram. Soc.* **72** (1987) 171.
2. N. KIKUCHI and H. YOSHIMURA, *New Diamond* **3**(3) (1988) 26.
3. M. S. WONG, R. MEILUNAS, T. P. ONG and R. R. H. CHANG, *Appl. Phys. Lett.* **54** (1989) 2006.
4. C. P. CHANG, D. L. FLAMN, D. E. IBBOTSON and J. A. MUCHA, *J. Appl. Phys.* **63** (1988) 1744.
5. I. WATANABE and K. SUGATA, *Jpn J. Appl. Phys.* **27** (1988) 1397.
6. R. MEILUNAS, M. S. WONG, K. C. SHENG, R. P. H. CHANG and R. P. VAN-DUYNE, *Appl. Phys. Lett.* **54** (1989) 2204.
7. M. KAMO, Y. SATO, S. MATSUMOTO and N. SETAKA, *J. Crystal Growth* **62** (1983) 642.
8. M. KAMO, Y. SATO and N. SETAKA, *Nippon Kagaku Kaishi* (1984) 1642.
9. Y. MITSUDA, Y. KOJIMA, T. YOSHIDA and K. AKASHI, *J. Mater. Sci.* **22** (1987) 1557.
10. C. F. CHEN, Y. C. HUANG and S. HOSOMI, *Hyomen Gijutsu* **39** (1988) 434.
11. K. HIGUCHI, S. NODA and O. KAMIGAITO, *Funtai-Oyobi-Funmatsu-Yakin* **36** (1989) 139.
12. J. S. MA, H. KAWARADA, T. YONEHARA, J. SUZUKI, J. WEI, Y. YOKOTA and A. HIRAKI, *Appl. Phys. Lett.* **55** (1989) 1071.
13. H. SUZUKI, H. MATSUBARA and N. HORIE, *Funtai-Oyobi-Funmatsu-Yakin* **33** (1986) 262.

Received 15 January

and accepted 19 November 1990